Nondipolarity of axial channeling radiation at GeV beam energies

W. Wagner,[1,*] A. A. Savchenko,[1,2,†] B. Azadegan,[3] and M. Shafiee[3]

[1]*National Research Nuclear University MEPhI, Kashirskoye sh. 31, 115409 Moscow, Russia*
[2]*National Research Centre "Kurchatov Institute", Akademika Kurchatova pl. 1, 123182 Moscow, Russia*
[3]*Hakim Sabzevari University, P.O. Box 397, Sabzevar, Iran*

(Received 12 February 2019; published 16 May 2019)

We consider the nondipolarity of axial channeling radiation generated in a tungsten single crystal at electron-beam energies of several GeV. The calculations are based on the realistic axial continuous potential. It could be shown that, compared to the dipole approximation, the nondipole approximation results in a considerable variation of the channeling radiation spectrum. In a simulation of positron production via conversion of γ radiation into e^+e^- pairs, the observed effect may play an important role.

DOI: 10.1103/PhysRevAccelBeams.22.054502

I. INTRODUCTION

Assessing today, it is really remarkable that the phenomenon of channeling of charged particles (ions) when moving through a single crystal along selected directions (crystallographic planes or axes) was discovered by means of computer simulations in 1963 [1]. Shortly later, the effect was confirmed experimentally in 1964 [2] and was explained theoretically in 1965 [3].

Governed by the so-called continuous planar or axial potential [3], the classical description of channeling of relativistic light charged particles (electrons or positrons) results in a sinusoidal or, respectively, ellipsoidal motion which, consequently, leads to the emission of electromagnetic radiation. Figured out in 1976 [4,5], channeling radiation (CR) turned out to be an intense, tunable, nonconventional source of x and γ rays. After its observation in 1978 [6], CR was the object of numerous investigations; a comprehensive survey of them may be found in the extensive reference lists of relevant monographs [7–14].

While the first CR x-ray source was presented in Ref. [15], an interesting application of high-energy CR γ rays consists in their conversion into e^+e^- pairs to create an intense positron source for future e^+e^- colliders (see, e.g., Ref. [16]). An axially oriented tungsten (W) crystal serving at the same time as the radiator and converter was used at the KEKB factory in Ref. [17]. An advanced method, the so-called hybrid positron source, was proposed in Ref. [18] and has further been investigated in Refs. [19–21].

Based on realistic continuous potentials, we developed *Mathematica* [22] computer codes for the classical calculation of planar as well as axial CR valid at particle energies higher than about 100 MeV [23,24]. Dechanneling was evaluated in Ref. [25] (see also Refs. [26,27]) but first already applied for the simulation of positron production in a hybrid scheme in Ref. [28].

Classical CR calculations are based on the computation of particle trajectories in the continuous planar or axial potentials. For relativistic channeled particles, the longitudinal velocity $v_z \approx c$ (c means the velocity of light). Hence, the emission of CR is caused by their transverse motion. Over a rather large interval of particle energy, the transverse motion may be assumed to be quasi-independent on the longitudinal one and even nonrelativistic, which allows the calculation of CR in a dipole approximation [13]. This is valid if the energy of radiated photons is much smaller than the particle energy. The assumed condition successively weakens when the energy of the channeled particle approaches values near one GeV [13,29,30], which leads to remarkable changes of the photon spectrum and the CR intensity. As in general considered in Ref. [31] for the particle motion through a flat undulator, we calculated the effect of nondipolarity on planar electron CR in Ref. [32]. The present paper deals with axial electron CR in a nondipole approximation.

Theoretically, nondipolarity of axial CR is considered in Refs. [29,30,33–36]. The analytic approach of the problem is rather complicated and requires analog modeling (i.e., approximation) of the continuous axial potential. The numerical treatment applied in Ref. [31] as well as in the present paper enables one to solve the equations of motion for realistic periodic continuous (planar or axial) potentials given in their most common 1D or 2D form, respectively [37].

*Corresponding author.
w.wagner@hzdr.de
†Corresponding author.
aasavchenko1@mephi.ru

Spectral-angular and energy distributions of CR are then calculated using classical electrodynamics [38].

Since the axial continuous potential is mostly deeper than the planar one, axial CR in a W crystal was preferred to the planar one in Refs. [17–21]. Therefore, we also restrict our calculations to a W single-crystal radiator, because, due to its large atomic number, the CR yield is expected to be larger than that for diamond, Si, or Ge crystals.

II. COUPLED MOTION OF THE CHANNELED PARTICLE

By analogy with the nondipole approximation applied for planar channeling in Ref. [32], we consider the coupling of longitudinal and transverse motion at axial channeling by adding the two transverse velocity components v_x and v_y to the equation of motion of the relativistic channeled particle:

$$\frac{d\mathbf{p}}{dt} = \frac{d}{dt}\left(\frac{m\mathbf{v}}{\sqrt{1-\frac{v_x^2+v_y^2+v_z^2}{c^2}}}\right), \tag{1}$$

where m is the electron rest mass, $\mathbf{p}$ is the electron momentum, $\mathbf{v}$ is the particle velocity, and v_z is its longitudinal component.

For $v_{x,y} \ll v_z \approx c$, one obtains the equations of particle motion [24]:

$$\gamma m\ddot{x} = \mathbf{F}_x = -\frac{\partial U(x,y)}{\partial x}, \tag{2}$$

$$\gamma m\ddot{y} = \mathbf{F}_y = -\frac{\partial U(x,y)}{\partial y}, \tag{3}$$

$$\gamma m\ddot{z} = \mathbf{F}_z = 0, \tag{4}$$

where $\gamma = 1/\sqrt{1-\beta^2}$ means the Lorentz factor and $\beta = v/c$.

The realistic continuous potential for axial electron channeling reads [24]

$$U(x,y) = \sum_g u_g e^{i\mathbf{g}\cdot\mathbf{r}_\perp}, \tag{5}$$

$$u_g = -\frac{2\pi}{V_c} a_0 e^2 \sum_{i=1}^{4} \alpha_i e^{-\frac{1}{4}(\frac{\beta_i}{4\pi^2}+2\rho^2)g^2}, \tag{6}$$

where the vector $\mathbf{g} = \mathbf{g}_m$ represents all m reciprocal lattice vectors perpendicular to the axis considered, $\mathbf{r}_\perp$ is the radius vector in cylindrical coordinates, u_g denotes m Fourier coefficients, ρ is the mean-squared thermal-vibration amplitude, a_0 is the Bohr radius, V_c is the volume of unit cell, and α_i and β_i are coefficients of potential approximation after Ref. [37]. The continuous potential of the $\langle 100\rangle$ axis of a W single crystal is depicted in Fig. 1.

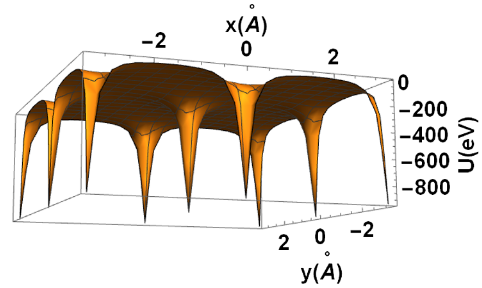

FIG. 1. Realistic continuous potential of the $\langle 100\rangle$ axis of a W single crystal for electron channeling.

The condition $dp_z/dt = 0$ is necessary to obtain a convergent solution of the equations of motion. The nondipole approximation supposes that the coupling of transverse and longitudinal velocities is contained in the Lorentz factor

$$\gamma = \frac{1}{\sqrt{1-\frac{v_x^2+v_y^2+v_z^2}{c^2}}}. \tag{7}$$

With given initial conditions at time $t = 0$, i.e., at the point of incidence into the crystal, one finds

$$v_z(t) = v_z(0)\left[1-\frac{1}{2c^2}\{[v_x^2(t)+v_y^2(t)]-[v_x^2(0)+v_y^2(0)]\}\right]. \tag{8}$$

From Eqs. (2) and (3), one obtains the transverse velocities $v_x(t)$ and $v_y(t)$ and trajectories $x(t)$ and $y(t)$ as well. This allows one to solve Eq. (8) for $z(0) = 0$. Integration of $v_z(t)$ gives $z(t)$:

$$z(t) = \int_0^t v_z(t')dt' = v_z(0)\left(1+\frac{1}{2c^2}[v_x^2(0)+v_y^2(0)]\right)t - \frac{v_z(0)}{2c^2}\int_0^t [v_x^2(t)+v_y^2(t)]dt. \tag{9}$$

Here, the second part in Eq. (9) represents a longitudinally oscillating term.

The longitudinal velocity averaged over one oscillation period T is

$$\langle\dot{z}\rangle = \frac{\bar{\beta}_z}{c} = \frac{1}{cT}\int_0^T \dot{z}(t)dt. \tag{10}$$

Finally, the trajectory of the channeled electron reads

$$\mathbf{r}(t) = x(t)\mathbf{e}_x + y(t)\mathbf{e}_Y + [\bar{\beta}_z ct + z(t)]\mathbf{e}_Z, \tag{11}$$

where $x(t)$, $y(t)$, and $z(t)$ are periodic with period T and $T/2$, respectively.

From now on, we change to spherical coordinates:

$$\mathbf{n} = \sin(\theta)\cos(\phi)\mathbf{e}_x + \sin(\theta)\sin(\phi)\mathbf{e}_y + \cos(\theta)\mathbf{e}_z. \quad (12)$$

The unit vector $\mathbf{n}$ points in the direction of photon emission.

III. NONDIPOLARITY OF AXIAL CR

Obtained the trajectory of the channeled electron in the approximation of coupled motion, one can calculate the spectral-angular distributions of CR by applying classical electrodynamics if the photon energy is sufficiently small compared to the particle energy:

$$\frac{d^2E}{d\omega d\Omega} = \frac{e^2}{4\pi^2 c}\left|\int_0^\tau e^{i(\omega t - \mathbf{k}\cdot\mathbf{r})}\frac{\mathbf{n}\times[(\mathbf{n}-\boldsymbol{\beta})\times\dot{\boldsymbol{\beta}}]}{(1-\boldsymbol{\beta}\mathbf{n})^2}dt\right|^2, \quad (13)$$

where $c\boldsymbol{\beta} = \dot{\mathbf{r}}$, $\mathbf{k} = \omega\mathbf{n}/c$ is the wave vector of radiation with frequency ω, and $\tau = NT$ means the time for traversing the crystal, during which the particle executes N transverse oscillations.

To obtain the CR spectrum for a real electron beam, averaging over all incidence points into the crystal (means over all possible trajectories) and integration over the solid angle $d\Omega = \sin\theta d\theta d\varphi$ must be performed. The total energy spectrum of CR is obtained by restricting the observation angle to $\theta \leq 1/\gamma$. All corresponding calculations have been carried out numerically. For that, we adopted our computer code developed for planar channeling to the axial case (cf. Refs. [32,39]). Under the assumption that the number of transverse oscillations in the crystal is large enough, one may express Eq. (13) per unit crystal thickness.

The integration over all emission angles has to be performed using the relation

$$\omega = \frac{\omega_n}{(1-\bar{\beta}_z\cos\theta_m)}. \quad (14)$$

Finally, the spectral distribution of CR per unit crystal thickness reads

$$\frac{d\bar{E}}{d\hbar\omega} = \frac{e^2\omega}{2\pi\hbar c^2}\sum_{n=1}^{\infty} I_n(\theta_m), \quad (15)$$

where $I_n(\theta_m) = |a_n|^2 - |\mathbf{n}\mathbf{a}_n|$, $\omega_n = 2\pi n/T$,

$$\mathbf{a}_n = \frac{1}{T}\int_0^T \boldsymbol{\beta}(t)e^{-i\frac{\omega}{c}\mathbf{n}(\varphi,\theta)\cdot\mathbf{r}(t)}e^{i\omega_n t}dt, \quad (16)$$

and the photon frequencies are restricted by the condition

$$\omega_{\min} = \frac{\omega_n}{1+\beta} \leq \omega \leq \frac{\omega_n}{1-\beta} = \omega_{\max}. \quad (17)$$

IV. RESULTS OF CALCULATIONS

In what follows, we present a comparison of trajectories of channeled particles and CR spectra obtained in the dipole as well as in the nondipole approximation.

Figure 2 shows examples of projected on the $x-y$ plane transverse electron trajectories of axial channeling along the $\langle 100\rangle$ axis of a W single crystal calculated for a given incidence point at parallel incidence with respect to the crystal axis.

Channeling radiation spectra calculated in the dipole and nondipole approximation for electrons of energy 0.8, 2,

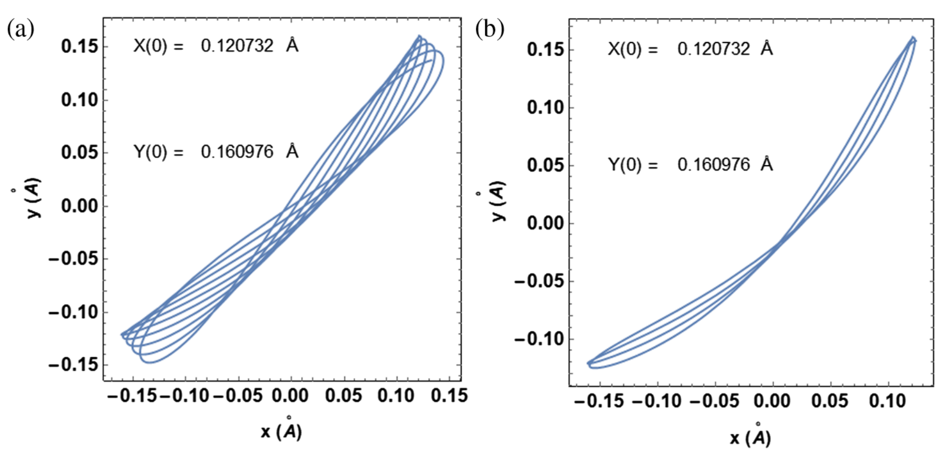

FIG. 2. Projected on the $x-y$-plane trajectories for 800 MeV electrons axially channeled along the $\langle 100\rangle$ axis of a W single crystal for parallel incidence at given coordinates $x(0)$, $y(0)$. (a) Five oscillation periods, (b) two oscillation periods.

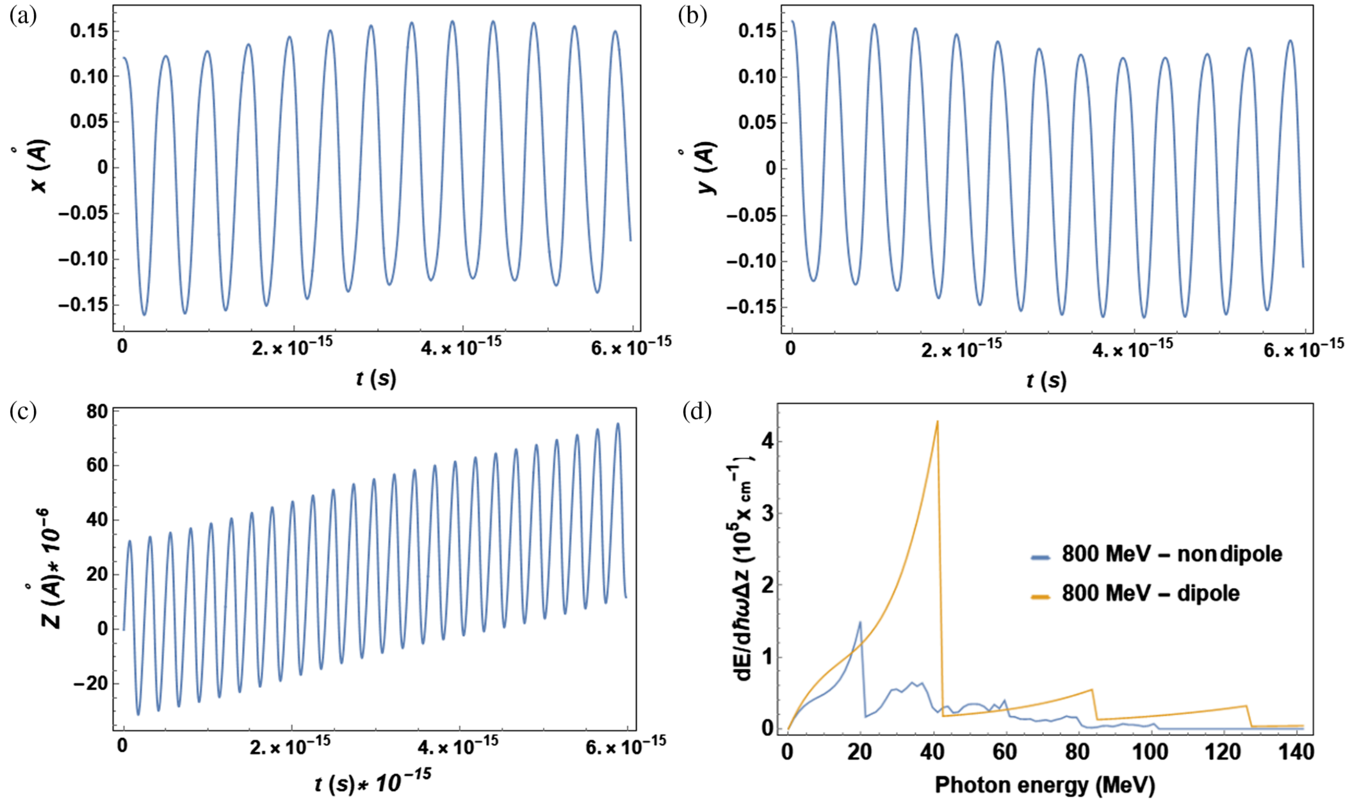

FIG. 3. Electron trajectories relating to the projections shown in Fig. 2. (a) $x(t)$, (b) $y(t)$, (c) $z(t)$. (d) Photon spectrum of one 800 MeV electron incident at the coordinates given in Fig. 2 and channeled along the $\langle 100 \rangle$ axis of a 20-μm-thick W single crystal. Dipole approximation (yellow line) and nondipole approximation (blue line).

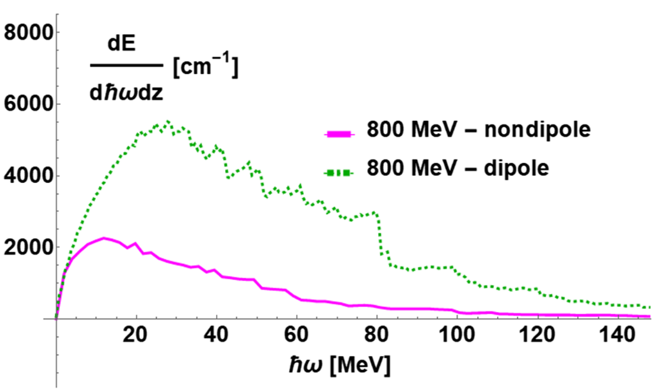

FIG. 4. Comparison of CR spectra calculated in the dipole and nondipole approximation for electrons of energy 800 MeV axially channeled along the $\langle 110 \rangle$ axis of a 20-μm-thick W single crystal at parallel incidence with respect to the crystal axis.

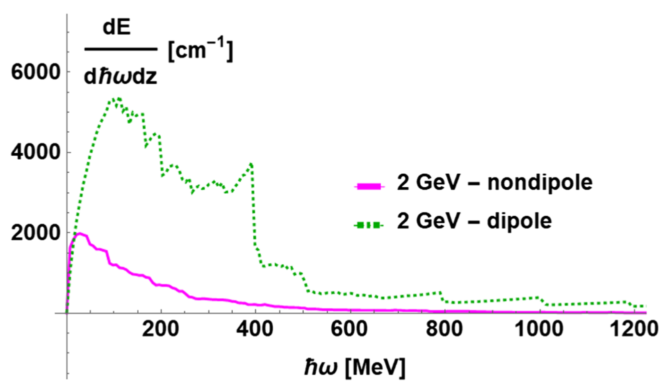

FIG. 5. Comparison of CR spectra calculated in the dipole and nondipole approximation for electrons of energy 2 GeV axially channeled along the $\langle 100 \rangle$ axis of a 20-μm-thick W single crystal at parallel incidence with respect to the crystal axis.

and 5 GeV channeled along the $\langle 100 \rangle$ axis of a 20-μm-thick W single crystal are shown in Figs. 4–6.

To not confuse the main issue of this paper, we for the present neglect dechanneling, although multiple scattering strongly diminishes the absolute CR output, if the crystal thickness is comparable with the dechanneling length [25]. With reference to analytic Fokker-Planck calculations of axial dechanneling [40], a rough estimation of the axial dechanneling length for a W crystal at an electron energy of 1 GeV gives several microns only. Numerical calculations using realistic potentials (cf. Refs. [25–27]) were unavailable up to now. Since dechanneling affects absolute values, the effect of nondipolarity of CR should principally hold.

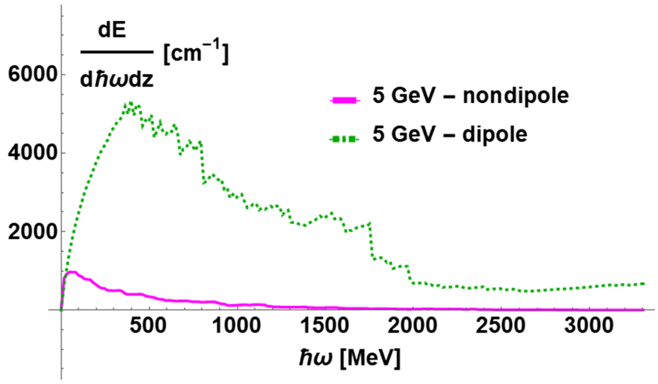

FIG. 6. Comparison of CR spectra calculated in the dipole and nondipole approximation for electrons of energy 5 GeV axially channeled along the ⟨100⟩ axis of a 20-μm-thick W single crystal at parallel incidence with respect to the crystal axis.

V. DISCUSSION OF OBTAINED RESULTS

The initial conditions for the projected trajectories shown in Fig. 2 are equally chosen. The example is a very simple one; more complicated trajectories are possible. Figure 2(b) accounting for the first two periods only is asymmetric, and spiraling proceeds not yet around the central axis. This is realized only after several periods as shown in Fig. 2(a), where five periods are depicted. Since radiation is caused by acceleration of the charged particle, asymmetric spiraling will only slightly influence the photon spectrum. Figures 3(a) and 3(b) illustrate the interplay of transverse trajectories. Figure 3(c) shows the doubled oscillation frequency in the longitudinal direction which is caused by the oscillating term in Eq. (9). This term induces radiation not directed into the forward cone $\theta \leq 1/\gamma$ but causing radiation losses.

Figures 4–6 reveal a striking difference between the CR spectra and intensities calculated in the dipole and nondipole approximation. When the photon energy of dipole radiation increases with an increasing beam energy as expected, the spectra obtained in the nondipole approximation shrink towards lower energy. In addition, the magnitudes of the nondipole spectra rapidly decrease with an increasing electron energy if compared with the dipole spectra.

Here it must be noted that, due to the 2D problem, satisfactory averaging over all possible electron trajectories is extremely computer-time consuming. It could only partly be provided by calculating for an ensemble of 1600 beam particles. Nevertheless, the main trends could be sufficiently demonstrated. Preliminarily concluding, it seems that, compared to planar channeling [32], the effect of nondipolarity of CR is more pronounced at axial CR.

VI. CONCLUSIONS

We for the first time investigated the effect of nondipolarity of axial electron CR at GeV beam energies, taking into account the realistic axial continuous potential of a W crystal. It could be shown that, at such particle energies, the dipole approximation for CR emission strongly overestimates the CR yield, as the CR spectrum and the CR intensity emitted in the beam direction are substantially modified by the coupling of longitudinal and transverse motion of axially channeled electrons.

Compared with the results obtained for the 1D case of planar CR in our previous work [32], it seems that the nondipole approximation for the 2D case of axial CR plays a more important role. Further investigations are necessary to obtain significant conclusions, e.g., for the application of high-energy CR to produce intense positron beams [28,41].

ACKNOWLEDGMENTS

The work was supported by the Ministry of Science and Higher Education of the Russian Federation, Grant No. 3.2621.2017/4.6, and the Competitiveness Program of National Research Nuclear University "MEPhI."

[1] M. T. Robinson and O. S. Oen, The channeling of energetic atoms in crystal lattices, Appl. Phys. Lett. **2**, 30 (1963).

[2] E. V. Kornelsen *et al.*, Penetration of Heavy Ions of keV Energies into Monocrystalline Tungsten, Phys. Rev. **136**, A849 (1964).

[3] J. Lindhard, Motion of swift charged particles, as influenced by strings of atoms in crystals, Phys. Lett. **12**, 126 (1964); Influence of crystal lattice on motion of energetic charged particles, K. Dan. Vidensk. Selsk. Mat. Fys. Medd. **34**, 30 (1965).

[4] M. A. Kumakhov, On the theory of electromagnetic radiation of charged particles in a crystal, Phys. Lett. **57A**, 17 (1976).

[5] M. A. Kumakhov and R. Weddel, Theory of radiation of relativistic channelled particles, Phys. Status Solidi B **84**, 581 (1977).

[6] I. I. Miroshnichenko, J. Murray, R. O. Avakian, and T. Ch. Fieguth, Experimental study of radiation of channeled relativistic positrons, JETP Letters **29**, 722 (1979); M. J. Alguard, R. L. Swent, R. H. Pantell, B. L. Berman, S. D. Bloom, and S. Datz, Observation of Radiation from Channeled Positrons, Phys. Rev. Lett. **42**, 1148 (1979).

[7] N. P. Kalashnikov, V. S. Remizovich, and M. I. Riazanov, *Collisions of Fast Charged Particles in Solids* (Atomizdat, Moscow, 1980) (in Russian).

[8] *Coherent Radiation Sources*, edited by A. W. Saenz and H. Ueberall (Springer, Berlin, 1985).

[9] M. A. Kumakhov, *Radiation of Channelled Particles in Crystals* (Energoatomizdat, Moscow, 1986) (in Russian).

[10] M. A. Kumakhov and F. F. Komarov, *Radiation from Charged Particles in Solids* (AIP, New York, 1989).

[11] M. A. Kumakhov and W. Weddel, *Radiation of Relativistic Light Particles during Interaction with Single Crystals* (Spektrum, Heidelberg, 1991).

[12] A. I. Akhiezer and N. F. Shul'ga, *High-Energy Electrodynamics in Matter* (Gordon and Breach, New York, 1996).

[13] V. N. Baier, V. M. Katkov, and V. M. Strakhovenko, *Elektromagnetic Processes at High Energy in Oriented Single Crystals* (World Scientific, Singapore, 1998).

[14] P. Rullhusen, X. Artru, and P. Dhez, *Novel Radiation Sources Using Relativistic Electrons* (World Scientific, Singapore, 1998).

[15] W. Wagner, B. Azadegan, M. Sobiella, J. Steiner, K. Zeil, and J. Pawelke, An intense channeling radiation source, Nucl. Instrum. Methods Phys. Res., Sect. B **266**, 327 (2008).

[16] F. Zimmermann, High-energy physics strategies and future large-scale projects, Nucl. Instrum. Methods Phys. Res., Sect. B **355**, 4 (2015).

[17] T. Suwada, M. Satoh, K. Furukawa, T. Kamitani, T. Sugimura, K. Umemori, H. Okuno, Y. Endou, T. Haruna, R. Hamatsu, T. Sumiyoshi, K. Yoshida, A. P. Potylitsyn, I. S. Tropin, and R. Chehab, First application of a tungsten single-crystal positron source at the KEK B factory, Phys. Rev. ST Accel. Beams **10**, 073501 (2007), and references therein.

[18] R. Chehab *et al.*, Study of a positron source generated by photons from ultra-relativistic channeled particles, in *Proceedings of the 1989 Particle Accelerator Conference, Chicago, IL* (IEEE, New York, 1989), p. 283.

[19] X. Artru, A simulation code for channeling radiation by ultrarelativistic electrons or positrons, Nucl. Instrum. Methods Phys. Res., Sect. B **48**, 278 (1990).

[20] X. Artru, R. Chehab, M. Chevallier, and V. Strakhovenko, Advantages of axially aligned crystals used in positron production at future linear colliders, Phys. Rev. ST Accel. Beams **6**, 091003 (2003).

[21] I. Chaikovska *et al.*, Optimization of a hybrid positron source using channeling, Nucl. Instrum. Methods Phys. Res., Sect. B **402**, 58 (2017).

[22] Mathematica©, https://www.wolfram.com/mathematica/.

[23] B. Azadegan and W. Wagner, Simulation of planar channeling-radiation spectra of relativistic electrons and positrons channeled in a diamond-structure or tungsten single crystal (classical approach), Nucl. Instrum. Methods Phys. Res., Sect. B **342**, 144 (2015).

[24] B. Azadegan, S. B. Dabagov, and W. Wagner, Computer simulation of the radiation of electrons axially channeled in a thin Ge single crystal, Nucl. Instrum. Methods Phys. Res., Sect. B **269**, 2098 (2011).

[25] B. Azadegan, W. Wagner, A. A. Savchenko, and A. A. Tishchenko, Simulation of channeling radiation and positron production in thick diamond structures and a tungsten single crystal, Radiat. Phys. Chem. **157**, 84 (2019).

[26] H. Backe, P. Kunz, W. Lauth, and A. Rueda, Planar channeling experiments with electrons at the 855 MeV Mainz Microtron MAMI, Nucl. Instrum. Methods Phys. Res., Sect. B **266**, 3835 (2008).

[27] H. Backe, W. Lauth, and T. N. Tran Thi, Channeling experiments at planar diamond and silicon single crystals with electrons from the Mainz Microtron MAMI, J. Instrum. **13**, C04022 (2018).

[28] B. Azadegan, S. A. Mahdipour, and W. Wagner, Simulation of positron energy spectra generated by channeling radiation of GeV electrons in a tungsten single crystal, J. Phys. Conf. Ser. **517**, 012039 (2014).

[29] A. I. Akhiezer and N. F. Shul'ga, *High-Energy Electrodynamics in Matter* (Nauka, Moskva, 1993) (in Russian).

[30] V. V. Beloshitsky and F. F. Komarov, Electromagnetic radiation of relativistic channeling particles (the Kumakhov effect), Phys. Rep. **93**, 117 (1982).

[31] A. P. Potylitsyn, *Electron Radiation in Periodic Structures* (NTL, Tomsk, 2009).

[32] B. Azadegan and W. Wagner, Non-dipolarity of channeling radiation at GeV beam energies, Nucl. Instrum. Methods Phys. Res., Sect. B **402**, 63 (2017).

[33] A. Bazylev, V. I. Glebov, and N. K. Zhevago, Spectral distribution of the radiation in planar and axial channeling of ultrarelativistic electrons, Sov. Phys. JETP **51**, 31 (1980).

[34] M. A. Kumakhov and Ch. G. Trikalinos, Higher harmonics of spontaneous radiation of ultrarelativistic channeled particles, Sov. Phys. JETP **51**, 815 (1980).

[35] R. Wedell, Electromagnetic radiation of relativistic positrons and electrons during axial and planar channelling in monocrystals, Phys. Status Solidi (b) **99**, 11 (1980).

[36] A. Bazylev and N. K. Zhevago, Electromagnetic radiation by channeled particles, Radiat. Eff. **54**, 41 (1981).

[37] P. A. Doyle and P. S. Turner, Relativistic Hartree–Fock x-ray and electron scattering factors, Acta Crystallogr. A **24**, 390 (1968).

[38] J. D. Jackson, *Classical Electrodynamics* (Wiley, New York, 1975).

[39] H. Salehi, B. Azadegan, and M. Shafeei, Dynamics of electron (positron) motion using a Fokker-Planck equation and of emission of radiation during planar channeling, Nucl. Instrum. Methods Phys. Res., Sect. B **433**, 43 (2018).

[40] V. V. Beloshitskii and M. A. Kumakhov, Multiple scattering of electrons in axial channeling, Sov. Phys. JETP **55**, 265 (1982).

[41] S. V. Abdrashitov, O. V. Bogdanov, S. B. Dabagov, Yu. L. Pivovarov, and T. A. Tukhfatullin, Total yield and spectra of positrons produced by channeling radiation from 0.1–1.6 GeV electrons, Nucl. Instrum. Methods Phys. Res., Sect. B **402**, 54 (2017).